







Cite this: *Lab Chip*, 2017, 17, 2294

Organs-on-Chips with combined multi-electrode array and transepithelial electrical resistance measurement capabilities†

Ben M. Maoz, ^{‡ab} Anna Herland, ^{‡a} Olivier Y. F. Henry, ^{‡a} William D. Leineweber, ^a Moran Yadid,^{ab} John Doyle,^{ab} Robert Mannix,^{ac} Ville J. Kujala,^{ab} Edward A. FitzGerald,^a Kevin Kit Parker^{ab} and Donald E. Ingber ^{*abc}

Here we demonstrate that microfluidic cell culture devices, known as Organs-on-a-Chips can be fabricated with multifunctional, real-time, sensing capabilities by integrating both multi-electrode arrays (MEAs) and electrodes for transepithelial electrical resistance (TEER) measurements into the chips during their fabrication. To prove proof-of-concept, simultaneous measurements of cellular electrical activity and tissue barrier function were carried out in a dual channel, endothelialized, heart-on-a-chip device containing human cardiomyocytes and a channel-separating porous membrane covered with a primary human endothelial cell monolayer. These studies confirmed that the TEER-MEA chip can be used to simultaneously detect dynamic alterations of vascular permeability and cardiac function in the same chip when challenged with the inflammatory stimulus tumor necrosis factor alpha (TNF- α) or the cardiac targeting drug isoproterenol. Thus, this Organ Chip with integrated sensing capability may prove useful for real-time assessment of biological functions, as well as response to therapeutics.

Received 14th April 2017,
Accepted 4th June 2017

DOI: 10.1039/c7lc00412e

rsc.li/loc

Introduction

Microfluidic cell culture models, known as Organs-on-Chips (Organ Chips), have emerged as new and effective *in vitro* tools for recapitulating human physiology and drug responses under controlled conditions.^{1–4} Utilizing recent advances in microengineering and microfluidics, these models can reconstruct a physiologically relevant microenvironment and allow precise control of secreted cellular signalling signals as well as external stimuli including mechanical cues and pharmaceutical compounds.¹ Unlike traditional *in vitro* cell models, Organ Chips allow for vascular-like perfusion through endothelium-lined microchannels, which is critical for mimicry of physiological functions and pharmacokinetic (PK) modeling.⁵ In light of the improvement of Organ Chips as pharmacologically relevant models, it becomes increasingly important to integrate relevant assessment methods into the systems because real-time read-out of *in vitro* systems can

provide spatially and temporally resolved high-content information on basal cell function and pharmacodynamic (PD) drug responses. Here, we leverage the microengineering methods that are used to fabricate Organ Chips to integrate multiple suitable sensor elements into these microfluidic culture devices.

This is particularly relevant in the study of electrically active cell constructs such as the myocardium and its response to inflammation before or during pharmacological treatment. For example, the Organ Chip approach can be used to engineer an endothelialized cardiac model where cardiomyocytes cultured in one microfluidic channel are separated by a thin semi-permeable membrane from a second, parallel, endothelium-lined vascular channel. For this particular arrangement, measuring field potentials of cardiomyocytes using multi electrodes array (MEA) and simultaneously quantifying endothelial cell layer barrier function by transepithelial electric resistance (TEER) can result in a greater understanding of heart pharmacodynamics (PD). However, even though Organ Chips enable new types of functional tissue units with several biological functionalities, there are no examples of microfluidic culture devices with integrated sensors that can simultaneously assess multiple cellular responses.

The direct measurement of electrical resistance over a tissue barrier using TEER is a fast, label-free and highly sensitive measurement of the barrier integrity and permeability.⁶

^a Wyss Institute for Biologically Inspired Engineering at Harvard University, Boston, MA 02115, USA. E-mail: don.ingber@wyss.harvard.edu

^b Harvard John A. Paulson School of Engineering and Applied Sciences, Cambridge, MA 02138, USA

^c Vascular Biology Program and Department of Surgery, Boston Children's Hospital and Harvard Medical School, Boston, MA 02115, USA

† Electronic supplementary information (ESI) available. See DOI: 10.1039/c7lc00412e

‡ Authors contributed equally.

TEER measurements reflect the ionic conductance of the paracellular junctions of a cellular monolayer and they provide a valuable metric for all types of epithelial tissues, including the endothelium that lines blood and lymph vessels. TEER measurements have been applied to measure cell layer permeabilities in Organ Chip models of blood–brain-barrier (BBB),^{7,8} intestine⁹ and lung,^{10,11} among others. Importantly, we and others, have shown that integrating electrodes in Organ Chips close to the cell monolayer combined with electric circuit modeling,^{8,12} gives accurate TEER values. Although frequently reported in literature, electric signals recorded using electrodes located in Organ Chips inlets and outlets, *i.e.* far from the cell monolayer, result in erroneous estimates of the TEER values. In order to extract realistic TEER values from such a measurement configuration, multiple measurements are needed to allow factoring in the effect of uneven current densities across the cell layers and the elaboration of a correction model.^{13,14}

Extracellular measurements of electric cell activity in the form of MEAs is an invaluable tool for assessment of function of excitable cells, such as neural and muscle cells.^{15,16} For cardiac *in vitro* models, assessment of firing frequency or contraction/beat rate, as well as field potential (FP) and its duration (FPD) and conduction velocity,¹⁷ can be directly related to human patient data, such as the QT interval in the heart's electrical cycle.^{18,19} While this method represents the gold standard for high-throughput electrophysiology *in vitro* cultures, there are very few examples of integration of MEAs into microfluidic Organ Chips. Recently, MEAs were integrated into a microfluidic device to record field potential and drug responses of a myocardium (without a vascular compartment) using a flow cell combined with a commercial MEA.²⁰ While this work clearly demonstrated the importance of integrating MEAs to study electroactive cell cultures, the commercial MEA configuration considerably limited the microfluidic cell culture system design to a simple flow cell of reduced geometry when, in fact, more elaborated channel designs are required to extract additional physiologically relevant information.

In this work, we demonstrate novel integration of the two measurement modalities – TEER and MEA – in one Organ Chip system, here applied to create an endothelialized myocardium. The system allows real time and simultaneous assessment of cell barrier function and electrical activity, and it is applicable to virtually any type of cultured electrically active cell. Here, using the TEER–MEA chip we could simultaneously study both the integrity of the endothelium and the electrical activity of heart cardiomyocytes. This dual capability is useful to assess both drug actions and biological processes, such as inflammation, which induce multiple changes at the tissue and organ (multi-tissue) level. We applied the system to measure changes in endothelial barrier function following addition of the inflammatory stimulus, TNF- α , while at the same time monitoring its effects on the adjacent cardiac tissue. Additionally, we measured cardiac tissue responses when applying delivery of isoproterenol through the

endothelial channel, a drug commonly used to treat bradycardia, thereby mimicking the vascular (systemic) drug administration.

Results and discussion

Device design

The TEER–MEA chip was designed to allow measurements of both TEER and extracellular field potential in a dual channel, microfluidic, Organ Chip culture device. The TEER–MEA chip is composed of optically clear PDMS polymer layers defining two parallel hollow microchannels (2 cm long \times 1 mm wide; the top and bottom channels were 0.4 and 1 mm high, respectively) separated by a porous (0.4 μm diameter; 4×10^6 pores per cm^{-2}) PET membrane (Fig. 1a and b). This design allows the culture of two cell populations with fluid connections and cellular interactions across the membrane. To enable precise TEER measurements and minimize noise, the TEER electrodes were positioned close to the cell monolayer. In addition, to measure the impedance of the cell monolayer, the electrodes were designed in a four-point probe configuration (2 electrodes above the cells and 2 beneath), which allows both excitation and measurement. The MEA design enables the use of all 64 electrodes inside the microfluidic chip in conjunction with a commercial MEA head stage (multi channel systems), which facilitates adjustment-free measurements. With these design constraints, the bottom substrate was glass with 64 patterned microelectrodes arranged as an array of 2×32 electrodes along the length of the PDMS main channel to capture the electroactivity of the cardiomyocytes at different locations. These electrodes were also connected to contact pads and the TEER bottom electrodes; the top substrate was polycarbonate with complementary TEER electrodes. The microfluidic channels were designed to apply low shear stress on the sensitive electrically active cardiomyocytes in the taller (1 mm) lower channel and higher shear stress in the shorter (0.4 mm), upper, vascular channel (Fig. 1 and ESI† Fig. S1a). For the applications explored here with equal flow rates (60 $\mu\text{L h}^{-1}$) in both channels (Fig. 1c and ESI† Fig. S2), the lower channel exhibited 6.25 times lower shear stress (6.8×10^{-4} dynes per cm^2 versus 4.3×10^{-3} dynes per cm^2) than the upper channel.²¹

Device fabrication

TEER–MEA chips with integrated electrodes were fabricated by combining standard photolithographic metal patterning and insulation processes, using plot cutting and molding to form the flow channels (Fig. 1a and b). To ensure bonding between the PDMS microfluidic layer and the silicon nitride, polycarbonate layer and PET membrane, we employed silane functionalization using amine (APTES) and epoxy (GLYMO) reactions.^{22–24} Stable monolayers of APTES can readily self-assemble onto oxidized silicon nitride *via* coupling of the silane moieties at the

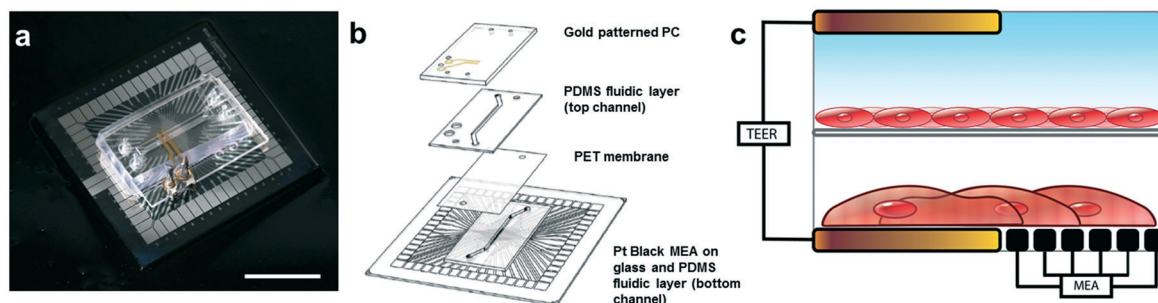


Fig. 1 TEER-MEA chip design – a. Photograph of the transepithelial electrical resistance–multi-electrode array (TEER-MEA) chip depicting the MEA connectors (platinum (Pt), in gray) the TEER electrodes (in gold) and the microfluidic chip on top of the MEA electrodes (scale bar 2.0 cm). b. Exploded view of the TEER-MEA chips showing the 5 layers of the device: MEA platform, first fluidic layer made of PDMS, followed by the PET membrane, top chip channel and TEER electrodes. c. Schematic of the experimental design – endothelial layer was grown on top of the PET membrane while cardiomyocytes were cultured on top of MEA. Both cell types were cultured between the two sets of TEER electrodes.

interface layer of silicon oxynitride produced during the oxidation process.²⁵ Similarly, APTES can assemble onto PET and PC, although monolayers are not typically obtained. Assembly occurs *via* interaction of the APTES amino end-group and the carboxylate residues produced at the surface of oxidized PET and PC.^{26,27} Bonding between epoxy-modified PDMS and amino-modified substrates normally occurred at room temperature within 10–20 minutes; however, we found that longer curing times at 60 °C were highly beneficial to obtain long-term stability. While bonding PDMS to PC or Si₃N₄ was more permissive for surface roughness, bonding PET to PDMS required that the PDMS layers to be extremely flat and homogeneous in thickness.

Electrode characterization

The impedance of the electrodes in a MEA will be directly affecting the field potential (FP) amplitude and the signal-to-noise ratio (S/N) of the signal from excitable cells. Using electroplating, platinum black (Pt black) was deposited on the microelectrodes (Fig. 2a and b) to increase the surface area of the recording microelectrodes, which considerably decreased their intrinsic impedance (Fig. 2c and d) and consequently their susceptibility to electrical noise. As native Pt black coatings are notoriously fragile, the plated electrodes were consecutively sonicated for 10 minutes in deionized water and isopropanol using a Branson 2510 ultrasonic cleaner (130 W, Danbury, USA). This process removed all weakly

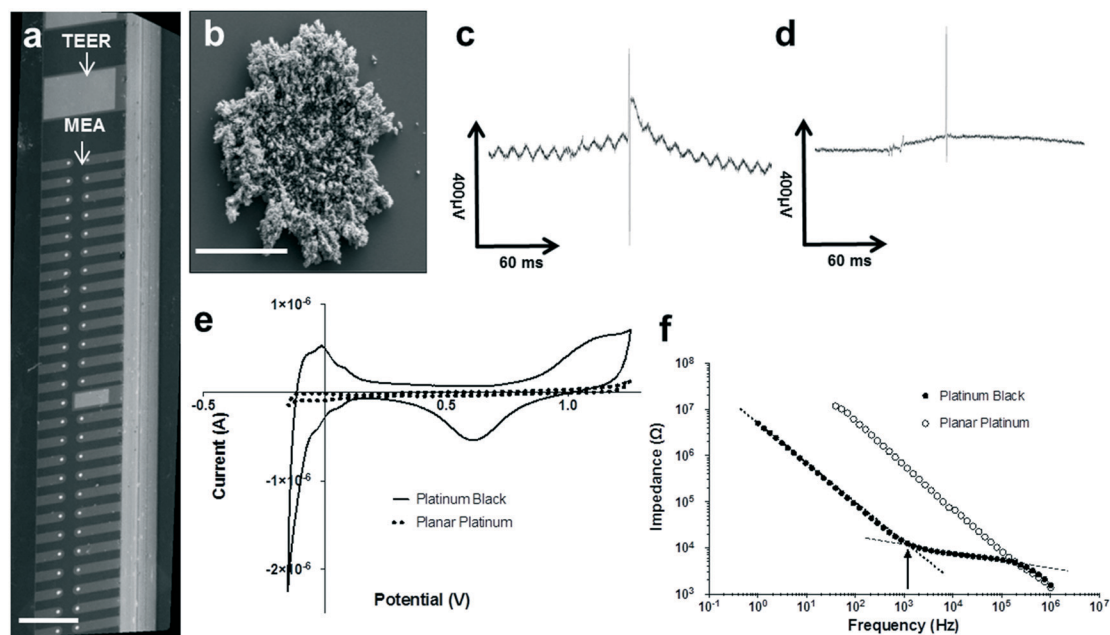


Fig. 2 MEA fabrication and characterization. a. Scanning electron microscope (SEM) image of the bottom layer electrodes. TEER electrodes (top) and MEA electrodes (bottom; scale bar – 500 μ m). b. Scanning electron microscope (SEM) image of one MEA electrode, in order to increase the S/N, MEAs were electroplated with Pt black increasing the surface area; scale bar – 30 μ m. c. and d. FP of cardiomyocytes measured from Pt electrodes (c) and Pt black electrode (d). The signal has 4 time higher S/N and less background effects. e. Cyclic voltammogram of Pt and Pt Black. f. Impedance spectroscopy, Pt black electrodes decrease the impedance values 3 orders of magnitude in comparison to regular Pt electrodes.

bound Pt black and the remaining Pt black was stable during the subsequent assembly steps and cell culture. The roughness factor, assessed by cyclic voltammetry in dilute sulfuric acid of the Pt black (Fig. 2e) was calculated to be 11.2 ± 0.87 . Scanning electron microscopy (SEM) revealed that the resulting Pt black outgrew the initial dimensions of the electrodes to a final diameter of $47.02 \pm 8.42 \mu\text{m}$ ($n = 10$). For comparison, the calculated roughness factor of the pristine Pt electrode was 1.46 ± 0.19 (Fig. 2b). In accordance with the inverse relation between the active electrode surface area and impedance, the increased surface roughness decreased the microelectrode impedance >40 times at the cut-off frequency of 1151 Hz (Fig. 2f), which is consistent with previous reports.²⁸

Baseline performance of the TEER–MEA Heart Chip

Endothelial cells that were introduced into the apical channel of the TEER–MEA chip formed a confluent monolayer within 24 hours of culture (ESI† Fig. S3a). Similarly, cardiomyocytes rapidly integrated into the basal channel of the chip and visual beating occurred within the adherent cells within 24 hours (ESI† Fig. S3b and Movie S1).

The basal transepithelial resistances of the devices are derived from the impedance spectroscopy and equivalent circuit diagram (Fig. 3a) to which the experimental data were fitted in order to extract TEER and capacitance values over the course of the experiments. The applicability of the selected equivalent circuit is illustrated by the high level of agreement between the model and data (Fig. 3a; goodness-of-fit χ^2 0.0087 ± 0.013 , *i.e.* $<10\%$ error). Using this approach, we found that the transepithelial resistance was significantly higher than background by 4 hours after cell seeding (Fig. 5a). The TEER values continued to increase steadily and stabilized at day 2, after which it averaged $232 \pm 47 \Omega$ for the following 4 days ($n = 12$), demonstrating the stability of the endothelium over the course of the experiment (Fig. 5a). This is also reflected in the capacitance measurement (Fig. 5b). The culture membrane capacitance decreased after seeding from $1190 \pm 194.63 \text{ nF}$ before seeding to $226 \pm 89 \text{ nF}$ at day 2 and it remained at this lower level during the rest of the experiment. Importantly, use of capacitance measurements in conjunction with TEER allowed us to follow culture mem-

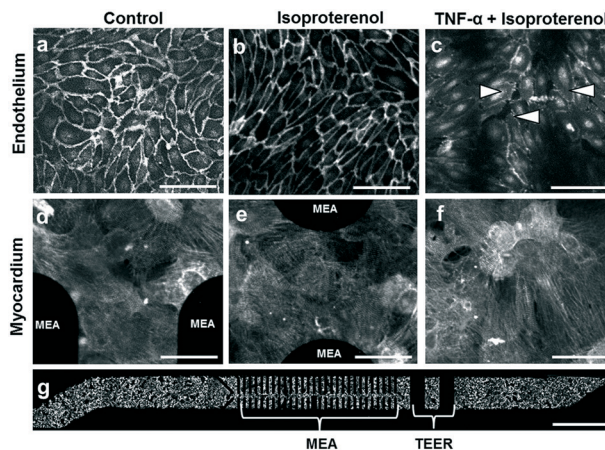


Fig. 4 Endothelial monolayer and myocardium in the device a–c. Immunocytochemistry of the confluent endothelial layer, vascular endothelial (VE)–cadherin was used to stain adherent cellular junctions. a. The non-treated control reveals a confluent endothelial layer, b. isoproterenol treatment did not show any change in the integrity of the barrier (supported with the TEER data), c. tumor necrosis factor- α (TNF- α) challenge, the barrier was damaged and holes can be observed leading to a decrease in the TEER values, (scale bar $10 \mu\text{m}$). d–f. Immunocytochemistry of myocardial tissue on the MEA (α -actinin). The cardiomyocytes did not show major changes between the control samples and drug addition (scale bar $10 \mu\text{m}$) g. Overview of the myocardial tissue that was formed in the lower channel of the chip (MEA compartment). The TEER and MEA electrodes can be seen in black (scale bar 5.0 mm).

brane coverage and cell adhesion, which reflects cell surface coverage, as previously reported.⁶

The first electrophysiological function of myocardium within the Heart Chip was detected 24 hours following cardiomyocyte seeding (Fig. 3b and c). Overall, the Pt black electroplating treatment improved the S/N by a factor of 4 in comparison to untreated platinum electrodes (Fig. 2c and d), which allowed us to unambiguously extract the required electrophysiological parameters to verify our system. The MEA measurement showed a basal average beat rate of 60 beats per minute and a basal rate-corrected field potential duration of $420 \pm 5 \text{ ms}$, which is the *in vitro* equivalent of the QT interval in the heart's electrical cycle. These values for the beat rate and field potential duration are similar to those previously reported for an engineered Heart Chip tissues without

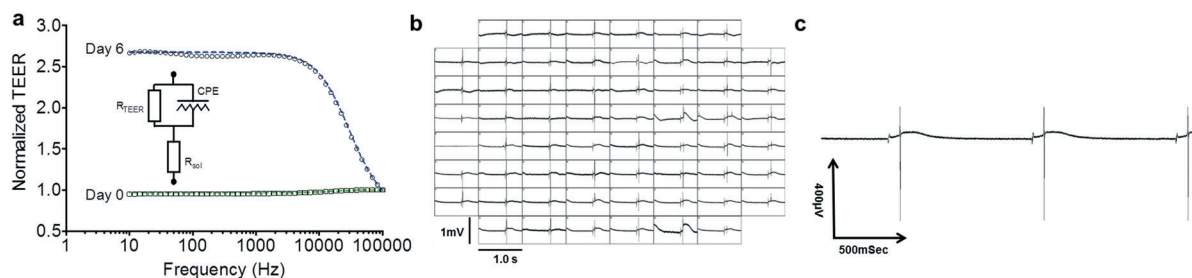


Fig. 3 TEER and MEA measurements a. Swipe impedance measurement over 100 kHz frequencies (black line) and data analysis (blue line). The TEER values are extracted by using the model (inset). MEA component b. Spontaneous beating recorded by the MEA arrays showing that all the electrodes are functional. c. MEA trace of single electrode.

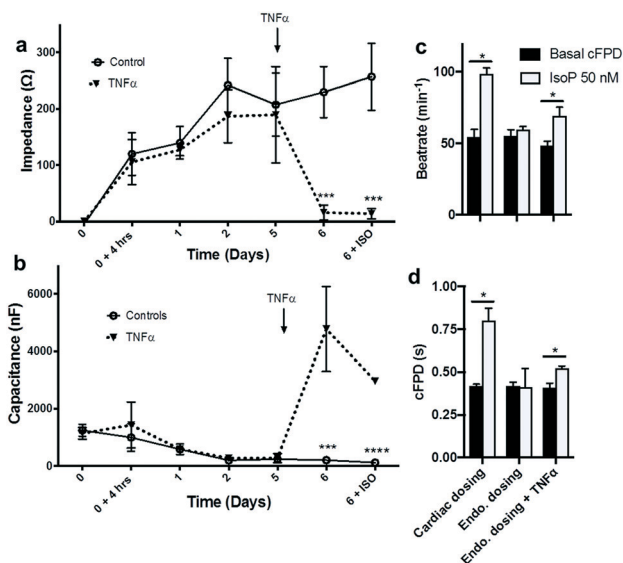


Fig. 5 Drug manipulation in the TEER-MEA chip TEER values of the endothelial layer were measured and calculated as described previously. a. The TEER (impedance) values develop over time due to the endothelial cell proliferation and the formation of a confluent layer. TNF- α was added at day 5 and the TEER values decreased to the same values as ECM-coated chips without cells, while the control sample showed maintained TEER. b. In contrary to the TEER (impedance) values, the capacitance demonstrated the opposite trend, the TNF- α addition increased the capacitance significantly. c. Isoproterenol infusion through the endothelial channel did not show a significant affect on the beat rate and corrected field potential duration (cFPD), whereas addition directly to the cardiomyocyte channel show an increase of both the beat rate by 80% (c) and the cFPD by 90% (d). Addition of isoproterenol through the endothelial channel treated by TNF- α show a significant increase of both the beat rate by 28% (c) and the cFPD by 42% (d).

an endothelium.^{19,20,29} In addition, MEA enabled us to calculate the conduction velocity *via* spatial analysis of the propagation of the electrical signal (ESI† Fig. S4). The human myocardium had a conduction velocity of $66.6 \pm 4.5 \mu\text{m ms}^{-1}$ which is similar to previously reported values for human cardiomyocytes.¹⁷

Impact of a TNF- α challenge on the TEER-MEA Heart Chip

TNF- α is a pro-inflammatory cytokine mainly produced by stimulated macrophages and monocytes in the systemic circulation. TNF- α has been shown to affect F-actin polymerization resulting in barrier degradation, clinically associated with endothelial dysfunction in both the pulmonary and cerebral microvasculature.^{30,31} When we added TNF- α ($2 \mu\text{g mL}^{-1}$) to the Heart Chip, we observed a significant ($p < 0.01$) disruption of the endothelial barrier with TEER values dropping from $230 \pm 45 \Omega$ to $15 \pm 13 \Omega$ after 24 hours (Fig. 5a). This decrease in TEER was also accompanied by an increase in capacitance from the low stable value of $194 \pm 33 \text{ nF}$ after day 2 to $2968 \pm 52 \text{ nF}$ after the chip was challenged with TNF- α (Fig. 5b). This is consistent with previous reports in which changes in cell capacitance were shown to correlate

with morphological changes of cells (Fig. 4), and increased values correlated with membrane folding and surface roughness.^{32–34} The severe damage to the endothelial barrier was further confirmed by using fluorescence microscopy, which revealed changes in the endothelial cytoskeleton and visual micro-gaps in the cellular junctions (Fig. 4c and ESI† Fig. S5 and S6). It is also noteworthy that we did not observe increased prevalence of pyknotic nuclei in the monolayer, suggesting that the TNF- α dose used here did not result in endothelial apoptosis (ESI† Fig. S5). TNF- α is also associated with cardiac disease and has been demonstrated to reduce contractility in hamster cardiomyocytes at 200 ng mL^{-1} .³⁵

Response of the TEER-MEA Heart Chip to isoproterenol

Isoproterenol is a non-selective β_1 -adrenergic agonist that is used clinically for the treatment of bradycardia. It also serves as a tool-box compound for characterizing physiological responses of *in vitro* heart models.^{19,28} We examined the effect on cardiomyocytes when isoproterenol was infused directly in the basal myocardial channel compared to the apical endothelial channel at control state and TNF- α challenge. When isoproterenol (50 nM) was infused into the basal myocardial channel, the beat rate increased by 80% (Fig. 5c, ESI† movie S2) while the cFPD (corrected field potential duration) rose by 90% (Fig. 5d). This correlates to the previously shown effects of isoproterenol of increased beat rate.^{19,28} However, when administrated to an intact endothelial channel no significant change in beat rate and cFPD could be seen. On the other hand the compromised, TNF- α challenged, endothelium permitted higher drug penetrance and 28% and 42% change for beat rate and cFPD respectively. In addition to monitoring changes in cardiac layer using the MEAs, TEER values were measured to determine whether isoproterenol alters the endothelial barrier (Fig. 5a and b). As expected, while the cardiomyocytes were highly affected by isoproterenol, the endothelial barrier was not affected by the drug (Fig. 5). It is important to note, that isoproterenol will eventually penetrate the endothelium, as occurs upon systemic vascular drug delivery *in vivo*. However, in the TEER-MEA chip, the intact endothelium significantly limited diffusion of the drug, which resulted in a longer response time compared to when the endothelium was disrupted (ESI† Fig. S7). Thus, this study demonstrates the advantage of the dual sensor system, which can monitor endothelial barrier function and electrical activity of the cardiomyocytes simultaneously in the same Organ Chip culture device.

Conclusions

The goal of the Organ Chip approach is not to engineer a fully functional living organ, but rather to reconstitute critical functions of major functional units of organs that cannot be currently modelled effectively using cell cultures or animal models, and to progressively add increasingly complex functionalities over time. Organ Chips offer major advantages over regular *in vitro* systems as they recapitulate relevant

tissue–tissue interactions, vascular perfusion, physical cues or organ–organ interactions that are known to be central to organ level function and ADME *in vivo*.^{4,5} However, there are still challenges and limitations that need to overcome. For example, it is necessary to create an endothelium-lined vasculature to mimic capillary permeability and enable *in vitro*-to-*in vivo* extrapolation of drug behaviors, as these devices are not full-sized organs. While some of these challenges still exist in our system, to our knowledge, this system is the first demonstration of a Heart Chip containing an endothelialized myocardium that allows direct assessment of barrier function and MEA measurements (Fig. 3 and 4 and ESI† Fig. S6). Vascularized heart models have been reported that demonstrate the self-organization of endothelium and myocardium, but they lack the ability to provide direct electrical assessment of organ function.¹⁸ A densely endothelialized Heart Chip model for drug evaluation was recently reported,³⁶ however unlike the chip reported here, this system relied on complex cell printing methods, as well as imaging strategies to determine beating frequency. In contrast, the integrated TEER and MEA electrodes reported here provide direct read-outs of these functions and hence, simplify data acquisition and interpretation considerably. Finally, it is important to note that we used the Heart Chip here only as a case study to demonstrate the dual sensing capabilities of our platform, which clearly have much broader potential applications. For example, this chip with fully integrated TEER and MEA capabilities also may be used to study drug penetrance combined with various vascular challenges in virtually any type of vascularized Organ Chip in the future.

Experimental

Chip design

The chip design was done with SolidWorks® software (Dassault Systèmes SolidWorks Corp. Waltham, MA, USA).

Chip fabrication

Microfluidic device. The microfluidic channels were cut in 1 mm and 0.4 mm polydimethylsiloxane (PDMS) films prepared by spin coating Sylgard 184® (Dow Corning, Midland, MI, USA) pre-mixed in 1:10 ratio with the curing agent onto acrylic discs followed by curing at 80 °C for 30 minutes. Fluidic designs were plot-cut and protected from air contaminant by a 100 µm thick PET film during subsequent processing and storage. The disc bearing the PDMS channels were finally laser cut into individual parts and stored under ambient conditions until further use.

Electrode patterning. The microelectrode arrays (MEAs) were fabricated using standard microfabrication procedures. Borosilicate glass wafers (University Wafers, Boston, MA, USA) were sequentially coated with lift-off resist LOR20A (Microchem Corp, Westborough, MA, USA, 3000 rpm, 60 seconds, softbake 180 °C for 4 minutes) and imaging resist S1805 (Microchem Corp, Westborough, MA, USA, 4000 rpm, 60 seconds, soft-bake 115 °C 1 minute). The MEA design

consisted of 57 micro-band electrodes 100 µm wide, one reference electrode 200 µm wide and two 1400 by 500 µm rectangular electrodes for TEER measurement. All electrodes were designed to align along the length of the microfluidic channel. This design was printed on transparency (Cad/art Services, Bandon, OR, USA), placed in hard-contact with the prepared wafer and exposed to UV light at 50 mJ cm² (@405 nm). The exposed resin was developed (CD-26 developer, 75 seconds) and wafers thoroughly rinsed with deionized water and dried under a stream of nitrogen. Following an O₂ plasma descum the prepared wafers were successively coated with titanium (10 nm) and platinum (90 nm) by e-beam evaporation (Denton, TX, USA) before lifting-off the resin in Remover-PG (Microchem Corp, Westborough, MA, USA, 60 minutes, 80 °C), rinsing with acetone and isopropanol and dried under a stream of nitrogen. Wafers were coated with 500 nm of silicon nitride (Si₃N₄) by PEVCD, then coated with resin S1818 (Microchem Corp, Westborough, MA, USA), 3000 rpm, 1 minute, followed by softbake 115 °C for 1 minute. Thereafter, contacts and electrode opening (MEA: 30 µm in diameter separated by 200 µm, reference electrode: 150 by 350 µm, TEER electrodes: two 450 by 750 µm electrodes separated by 500 µm) were patterned as previously described. The Si₃N₄ layer was finally etched by inductively coupled plasma reactive ion etching (SPP Process Technology Systems, Allentown, PA, USA), sonicated in acetone, rinsed in isopropanol and blow dried in a stream of nitrogen. Wafers were finally coated with a protective layer of S1818 before dicing and releasing individual MEAs.

Polycarbonate substrates (PC) 1 mm thick, were cut to size with their protective backing and inlets and outlets drilled as required. The protective backings removed, the polycarbonate substrates were rinsed with isopropanol, dried under a stream of compressed air and activated in oxygen plasma for 2 minutes (Technics Inc. Racine, WI, USA, 20 SCCM O₂, 300 mT). The electrode patterns were laser cut in silicon-coated paper backing and consisted in two 1 mm wide electrodes separated by 0.5 mm. The silicon-side of the resulting paper shadow masks were gently applied on the activated polycarbonate substrates using a homemade alignment jig. These substrates were sequentially coated with 3 nm of titanium and 25 nm of gold in a metal e-beam evaporator (Denton EE4, TX, USA). The paper shadow masks were finally gently peeled off the polycarbonate substrates before chemical activation.

MEAs were exposed to piranha solution (3:1; H₂SO₄ conc: 30% H₂O₂) for 1 minute before being sonicated in deionized water for 10 minutes and dried under a stream of compressed air. Electrodeposition of platinum black was performed in a custom-made electroplating set-up comprising of all the required external connections and an open cell. All microelectrodes were short-circuited and electrochemically activated in 2 M H₂SO₄ by cyclic voltammetry in the potential range -0.2 V to +1.5 V (100 scans, 1 V s⁻¹). Arrays were rinsed in deionized water and exposed to the Pt black plating solution (3.5% H₂PtCl₆ and 0.005% lead acetate

in deionized water). The Pt black solution was prepared fresh and sonicated for 10 minutes before use. Platinum black was electro-deposited on all electrodes in a single step by applying 5 consecutive -0.1 V 60 seconds pulses. The MEAs were finally successively sonicated for 10 minutes in deionized water and isopropanol using a Branson 2510 ultrasonic cleaner (130 W, Danbury, USA) to remove any weakly bound Pt black. The resulting electrodes were characterized electrochemically and by field emission SEM (Zeiss Ultra55, USA).

Device assembly. Before derivatization, MEAs were cleaned in acetone, sonicated in isopropanol and blow dried in a stream of nitrogen. Cleaned MEAs, PC substrates and PDMS layers were activated in an oxygen plasma (Technics Inc. Racine, WI, USA, 20 SCCM O_2 , 300 mT) before being immersed for 20 minutes in a 5% aqueous solution of APTES (Sigma-Aldrich, St Louis, MO, USA) (MEAs and PC) and a 1% aqueous solution of GLYMO (Sigma-Aldrich, St Louis, MO, USA) (PDMS). MEAs, PC and PDMS substrates were rinsed in water and dried under a stream of compressed air. MEAs/PDMS and PC/PDMS were aligned and brought into contact, gently pressed together to ensure conformational contact and baked at 60 °C overnight. These assembled MEA/PDMS and PC/PDMS parts (Fluidics parts) were plasma activated together with laser cut PET membranes (IP4IT, Louvain-la-Neuve, Belgium, 0.4 μ m pore diameter). Activated fluidic parts and PET membranes were immersed for 20 minutes in a 1% aqueous solution of GLYMO and a 5% aqueous solution of APTES respectively to introduce epoxy group at the surface of the PDMS layers and amino groups at the surface of the PET membrane. Fluidic parts and membranes were rinsed in water and dried in a stream of compressed air and finally aligned and brought in contact, gently pressed together to ensure conformational contact and baked at 60 °C overnight.

Cell culture

Human cell source and culture. Human umbilical cord vascular endothelial cells (Lonza, Walkersville, MD, USA) were expanded in EGM media (Lonza, Walkersville, MD, USA) and used at passage p2–p6 in the chip experiments. Human induced pluripotent stem cell-derived cardiomyocytes (hiPSC-CMs, Cor.4 U, Axiogenesis, Köln, Germany) were handled according to the vendor's instructions and used at passage 1 after thawing. Briefly, cryopreserved cells were thawed on fibronectin-coated cell culture vessels in the presence of 5 mg mL^{-1} puromycin (Sigma-Aldrich, St Louis, MO, USA) to select for MYH6-positive cells. Three hours after thawing the puromycin containing media was gently refreshed to wash out remaining cryopreservant (DMSO). Twenty-four hours after seeding cell culture media was refreshed without puromycin. The following day the cardiomyocytes were replated into the chips.

Chip culture. The TEER–MEA chips were surface treated in an oxygen plasma (Atto, Diener electronic GmbH, Germany, O_2 , 15 sccm, 100 W, 30 seconds) to create hydrophilic, sterile, flow systems. Both apical and basal channels were

coated overnight with human fibronectin (Sigma-Aldrich, St Louis, MO, USA) at 100 μ g mL^{-1} in PBS with Mg^{2+} and Ca^{2+} at 4 °C. Human umbilical cord vascular endothelial cells (HUVECs) were seeded at 2×10^6 cells per mL in the apical channel and left static overnight. Cardiomyocytes were seeded at 2×10^6 cells per mL in the basal channel, followed by 3 hours to overnight inculcation, before connecting both channels to flow at 60 μ L h^{-1} . Flow was controlled by a peristaltic pump (Ismatech, Cole-Parmer GmbH) and connections were in Pharmed tubing (Cole-Parmer, Vernon Hills, IL, USA) 0.511' inner diameter. Upon formation of a complete endothelial monolayer, the FBS content in the endothelial media was decreased from 2 to 0.5% and the cardiac media was switched to a serum free composition (Fig. 4a, d and g). To challenge the endothelial barrier, TNF- α (Sigma-Aldrich, St Louis, MO, USA) was added at 2 μ g mL^{-1} in the endothelial channel during overnight flow. Isoproterenol (Sigma-Aldrich, St Louis, MO, USA) 50 nM was added to the channels for 10 minutes. This 2-channel microfluidic chip enables perfusion either through both channels, or only on the endothelial side. But in this study, the endothelium and myocardium were continuously perfused with different tissue-specific medium—one mimicking interstitial fluid to support the myocardial cell function and the other acting as a blood substitute to maintain endothelial viability.

Device characterization and measurements

TEER measurements. TEER measurements were carried out by applying a 10 μ A sinusoidal excitation signal in a four-electrode setup in the frequency range 100 kHz–10 Hz. AC measurements are preferable for TEER measurements to avoid charging effects over the cell membranes and the electrodes.⁶ The TEER and capacitance values were derived using the equivalent circuit and model depicted in Fig. 3a and ESI† Fig. S1. A resistor R_{sol} describes the solution conductivity, while the electric response of the endothelial layer can be modelled using a resistor (RTEER) and a constant phase element (CPE) in parallel to extract TEER of the cell-cell junctions as well as the contribution of cell membrane capacitance and indirectly, overall monolayer surface area.

The mathematical expression of the CPE impedance is:

$$Z_{CPE} = \frac{1}{Y_0(j\omega)^n} \quad (1)$$

in which the impedance of the CPE is expressed as a function of the admittance Y_0 and an exponent n equaling 1 or 0 for an ideal capacitor or an ideal resistor respectively of the whole system. The capacitance of the cell layer C_{cell} was calculated from Z_{CPE} using eqn (2).

$$C_{cell} = \frac{(Y_0 \times R_{TEER})^{\frac{1}{n}}}{R_{TEER}} \quad (2)$$

MEA characterization

The impedance of the plain Pt and Pt black-modified microelectrodes were characterized using electrochemical impedance spectroscopy in the frequency range 1 MHz–1 Hz using a PGStat 128 N (Metrohm AG, Netherlands) using single sine excitation signals 5 mV in amplitude applied at the open circuit potential against an Ag/AgCl(sat KCl) reference electrode. Surface area and roughness factor of the microelectrodes were extracted from cyclic voltammograms recorded in the range -0.2 V to 1.25 V vs. Ag/AgCl(sat KCl) in 2 M sulfuric acid at a scan rate of 1 V s^{-1} . Charges associated with hydrogen absorption were translated into an area using 208 $\mu\text{C cm}^{-2}$ as conversion factor.³⁷ Roughness factors were calculated by dividing the calculated real electrochemical surface area by the electrode geometrical area (7.1×10^{-6} cm^2).

MEA measurement

Spontaneous cardiac field potentials (FPs) were recorded from cardiomyocytes using Pt and Pt Black microelectrode arrays (including ground electrodes) using the commercial multi-channel-system (USB-MEA60-Inv-BC-system, multi-channel-systems (MCS) GmbH, Germany). Cardiac FPs were recorded for 120 seconds for each measurement using Cardio2D software and analyzed with Cardio2D+ (both from multi channel systems). Measured parameters (FP duration [FPD, ms], peak-to-peak interval [PPI, s], beating rate [beats per minute], and conduction velocity [CV, cm per second]) were exported into MS Excel files for further analysis. FPD was corrected using the Fridericia's formula, $\text{cFPD} = \text{FPD}/\text{PPI}^{(1/3)}$, where cFPD is the rate-corrected FPD.

Immunocytochemistry. Chips were rinsed in phosphate-buffered saline and fixated in 4% paraformaldehyde (Sigma-Aldrich, St Louis, MO, USA) for 15 minutes at room temperature. Immunocytochemistry was carried out after permeabilization in phosphate-buffered saline with 0.05–0.1% Triton X-100 (Sigma-Aldrich, St Louis, MO, USA) and blocking for 30 minutes in 3–5% Bovine Serum Albumin (Jackson ImmunoResearch, West Grove, PA, USA) or 10% goat serum in phosphate-buffered saline with 0.05–0.1% Triton-X 100. Primary antibodies were applied in 2% goat serum or 0.5% BSA over-night at 4 °C or at room temperature. The following primary antibodies were used for immunocytochemistry experiments: mouse anti-vascular endothelial (VE)-cadherin (Abcam, Cambridge, UK, 1:100), alpha-actinin (Abcam, Cambridge, UK, 1:200) cells were washed three times in phosphate-buffered saline with 0.05–0.1% Triton-X 100, followed by staining with secondary antibody staining for 30–60 minutes at room temperature. The secondary antibodies were anti-rabbit or anti-mouse IgG conjugated with Alexa Fluor-488, Alexa Fluor-555, or Alexa Fluor-647 (Invitrogen, Carlsbad, CA, USA). Hoechst (10 mg mL^{-1} , Invitrogen, Carlsbad, CA, USA) was used at a dilution of 1:5000 for nuclei staining and Phalloidin-647 (Invitrogen, Carlsbad, CA, USA) was used for f-actin staining. Imaging was carried out in an Olympus confocal microscope (Olympus, Center Valley, PA,

USA) with appropriate filter cubes. Image processing was done in FIJI.³⁸

Conclusions

This work describes the first demonstration of a microfluidic device with integrated TEER electrodes and MEA arrays on the same chip to enable the simultaneous measurements of electrical activity, barrier function, and conformational changes of the cell monolayers. The chip allows simultaneous recording of drug effects and biological processes, here demonstrated with the pro-inflammatory TNF- α and the well characterized β 1 adrenergic receptor agonist isoproterenol. Moreover, we integrated a signal-enhancing electroplating step in the multi-electrode fabrication, which is especially well suited for future use of this chip with cells generating weaker electric signals. Thus, the TEER-MEA Heart Chip described in this study is a novel design that enables direct electrical assessment of an endothelialized myocardium. This new chip paves the way for more complex real-time assessment of cardio-toxicity and vascular effects of novel drugs in the Heart Chip configuration. However, it also opens up the possibility of carrying simultaneous analysis of the blood-brain barrier and neural tissues, as well as similar functional analysis of virtually any other Organ Chip system.

Competing financial interests

D. E. I. holds equity in Emulate, Inc., consults to the company, and chairs its scientific advisory board.

Acknowledgements

This research was sponsored by the Wyss Institute for Biologically Inspired Engineering at Harvard University and the Defense Advanced Research Projects Agency under Cooperative Agreement Number W911NF-12-2-0036. The views and conclusions contained in this document are those of the authors and should not be interpreted as representing the official policies, either expressed or implied, of the Defense Advanced Research Projects Agency, or the U.S. Government. This work was performed in part at the Center for Nanoscale System (CNS), a member of the National Nanotechnology Coordinated Infrastructure Network (NNCI), which is supported by the National Science Foundation under NSF award no. 1541959. CNS is part of Harvard University. We acknowledge the technical assistance of M. Rosnach and B. Fountaine.

Notes and references

- 1 E. W. Esch, A. Bahinski and D. Huh, *Nat. Rev. Drug Discovery*, 2015, **14**, 248–260.
- 2 M.-H. Wu, S.-B. Huang and G.-B. Lee, *Lab Chip*, 2010, **10**, 939–956.
- 3 A. K. Capulli, K. Tian, N. Mehandru, A. Bukhta, S. F. Choudhury, M. Suchyta and K. K. Parker, *Lab Chip*, 2014, **14**, 3181–3186.

- 4 S. N. Bhatia and D. E. Ingber, *Nat. Biotechnol.*, 2014, **32**, 760–772.
- 5 D. E. Ingber, *Cell*, 2016, **164**, 1105–1109.
- 6 B. Srinivasan, A. R. Kolli, M. B. Esch, H. E. Abaci, M. L. Shuler and J. J. Hickman, *J. Lab. Autom.*, 2015, **20**, 107–126.
- 7 L. M. Griep, F. Wolbers, B. De Wagenaar, P. M. Ter Braak, B. B. Weksler, I. A. Romero, P. O. Couraud, I. Vermes, A. D. Van Der Meer and A. Van Den Berg, *Biomed. Microdevices*, 2013, **15**, 145–150.
- 8 R. Booth and H. Kim, *Lab Chip*, 2012, **12**, 1784–1792.
- 9 H. J. Kim, H. Li, J. J. Collins and D. E. Ingber, *Proc. Natl. Acad. Sci. U. S. A.*, 2015, **113**, 201522193.
- 10 D. Huh, B. D. Matthews, A. Mammoto, M. Montoya-Zavala, H. Y. Hsin and D. E. Ingber, *Science*, 2010, **328**, 1662–1668.
- 11 F. R. Walter, S. Valkai, A. Kincses, A. Petneházi, T. Czeller, S. Veszelka, P. Ormos, M. A. Deli and A. Déry, *Sens. Actuators, B*, 2016, **222**, 1209–1219.
- 12 O. Y. F. Henry, R. Villenave, M. Cronce, W. Leineweber, M. Benz and D. E. Ingber, *Lab Chip*, 2017, DOI: 10.1039/C7LC00155J.
- 13 M. W. van der Helm, M. Odijk, J. P. Frimat, A. D. van der Meer, J. C. T. Eijkel, A. van den Berg and L. I. Segerink, *Biosens. Bioelectron.*, 2016, **85**, 924–929.
- 14 M. Odijk, A. D. van der Meer, D. Levner, H. J. Kim, M. W. van der Helm, L. I. Segerink, J.-P. Frimat, G. A. Hamilton, D. E. Ingber and A. van den Berg, *Lab Chip*, 2015, **15**, 745–752.
- 15 M. E. Spira and A. Hai, *Nat. Nanotechnol.*, 2013, **8**, 83–94.
- 16 M. Taketani and M. Baudry, *Advances in Network Electrophysiology Using Multi-Electrode Arrays*, 2006.
- 17 C. Denning, V. Borgdorff, J. Crutchley, K. S. A. Firth, V. George, S. Kalra, A. Kondrashov, M. D. Hoang, D. Mosqueira, A. Patel, L. Prodanov, D. Rajamohan, W. C. Skarnes, J. G. W. Smith and L. E. Young, *Biochim. Biophys. Acta, Mol. Cell Res.*, 2016, **1863**, 1728–1748.
- 18 O. Caspi, I. Itzhaki, I. Kehat, A. Gepstein, G. Arbel, I. Huber, J. Satin and L. Gepstein, *Stem Cells Dev.*, 2009, **18**, 161–172.
- 19 A. L. Lahti, V. J. Kujala, H. Chapman, A. P. Koivisto, M. Pekkanen-Mattila, E. Kerkelä, J. Hyttinen, K. Kontula, H. Swan, B. R. Conklin, S. Yamanaka, O. Silvennoinen and K. Alto-Setälä, *Dis. Models & Mech.*, 2012, **5**, 220–230.
- 20 V. Kujala, F. Pasqualini, J. Goss, J. Nawroth and K. K. Parker, *J. Mater. Chem. B*, 2016, **4**, 3534–3543.
- 21 Y. Son, *Polymer*, 2007, **48**, 632–637.
- 22 L. Tang and N. Y. Lee, *Lab Chip*, 2010, **10**, 1274–1280.
- 23 N. Y. Lee and B. H. Chung, *Langmuir*, 2009, **25**, 3861–3866.
- 24 K. S. Lee and R. J. Ram, *Lab Chip*, 2009, **9**, 1618–1624.
- 25 S. Watson, M. Nie, L. Wang and K. Stokes, *RSC Adv.*, 2015, **5**, 89698–89730.
- 26 C. Li and G. L. Wilkes, *J. Inorg. Organomet. Polym.*, 1997, **7**, 203–216.
- 27 A. Y. Fadeev and T. J. McCarthy, *Langmuir*, 1998, **14**, 5586–5593.
- 28 F. Heer, W. Franks, A. Blau, S. Taschini, C. Ziegler, A. Hierlemann and H. Baltes, *Biosens. Bioelectron.*, 2004, **20**, 358–366.
- 29 J. U. Lind, T. A. Busbee, A. D. Valentine, F. S. Pasqualini, H. Yuan, M. Yadid, S. Park, A. Kotikian, A. P. Nesmith, P. H. Campbell, J. J. Vlassak, J. A. Lewis and K. K. Parker, *Nat. Mater.*, 2017, **16**(3), 303–308.
- 30 C. Förster, M. Burek, I. A. Romero, B. Weksler, P.-O. Couraud and D. Drenckhahn, *J. Physiol.*, 2008, **586**, 1937–1949.
- 31 B. E. Dewi, T. Takasaki, I. Kurane and J. Virol, *Methods*, 2004, **121**, 171–180.
- 32 D. Opp, B. Wafula, J. Lim, E. Huang, J.-C. Lo and C.-M. Lo, *Biosens. Bioelectron.*, 2009, **24**, 2625–2629.
- 33 S. Michaelis, R. Robelek and J. Wegener, book chapter in *Tissue engineering III: cell-surface interactions for tissue culture*, 2012.
- 34 R. Lee, D. Hyun Jo, S. J. Chung, H.-K. Na, J. H. Kim and T. G. Lee, *Sci. Rep.*, 2016, **6**, 33668.
- 35 A. M. Feldman, A. Combes, D. Wagner, T. Kadakomi, T. Kubota, Y. Y. Li and C. Mctiernan, *J. Am. Coll. Cardiol.*, 2000, **35**, 537–544.
- 36 F. H. Moghadam, H. Alaie, K. Karbalaie, S. Tanhaei, M. H. Nasr Esfahani and H. Baharvand, *Differentiation*, 2009, **78**, 59–68.
- 37 J. M. Doña Rodríguez, J. A. Herrera Melián and J. Pérez Peña, *J. Chem. Educ.*, 2000, **77**, 1195.
- 38 J. Schindelin, I. Arganda-Carreras, E. Frise, V. Kaynig, M. Longair, T. Pietzsch, S. Preibisch, C. Rueden, S. Saalfeld, B. Schmid, J.-Y. Tinevez, D. J. White, V. Hartenstein, K. Eliceiri, P. Tomancak and A. Cardona, *Nat. Methods*, 2012, **9**, 676–682.